

# Effects of imidazolium-based ionic surfactants on the size and dynamics of phosphatidylcholine bilayers with saturated and unsaturated chains

Hwankyu Lee\*

Department of Chemical Engineering, Dankook University, Yongin 448-701, South Korea



## ARTICLE INFO

### Article history:

Received 10 March 2015

Received in revised form 4 April 2015

Accepted 22 May 2015

Available online 27 May 2015

### Keywords:

Imidazolium-based ionic surfactant

MD simulation

Lipid bilayer

## ABSTRACT

Imidazolium-based ionic surfactants of different sizes were simulated with 1,2-dimyristoyl-sn-glycero-3-phosphocholine (DMPC), 1-palmitoyl-2-oleoyl-sn-glycero-3-phosphocholine (POPC), and 1,2-dioleoyl-sn-glycero-3-phosphocholine (DOPC) bilayers. Regardless of the phospholipid type, larger surfactants at higher concentrations more significantly insert into the bilayer and increase the bilayer-surface size, in agreement with experiments and previous simulations. Insertion of surfactants only slightly decreases the bilayer thickness, as also observed in experiments. Although the surfactant insertion and its effect on the bilayer size and thickness are similar in different types of bilayers, the volume fractions of surfactants in the bilayer are higher for DMPC bilayers than for POPC and DOPC bilayers. In particular, ionic surfactants with four hydrocarbons yield their volume fractions of 4.6% and 8.7%, respectively, in POPC and DMPC bilayers, in quantitative agreement with experimental values of ~5% and ~10%. Also, the inserted surfactants increase the lateral diffusivity of the bilayer, which depends on the bilayer type. These findings indicate that although the surfactant insertion does not depend on the bilayer type, the effects of surfactants on the volume fraction and bilayer dynamics occur more significantly in the DMPC bilayer because of the smaller area per lipid and shorter saturated tails, which helps explain the experimental observations regarding different volume fractions of surfactants in POPC and DMPC bilayers.

© 2015 Elsevier Inc. All rights reserved.

## 1. Introduction

Room-temperature ionic liquids (ILs) are large organic or inorganic salts in the liquid phase at room temperature. Due to their low volatility, non-flammability, high conductivity, and thermal and chemical stability [1–5], they have been widely used for many industrial or environmental applications such as electrolytes and sorption media for catalysis [6,7], battery [8,9], separation process [10,11], synthesis of composite materials [12,13], and hydrolysis of cellulose [14]. However, recent experiments have shown that ILs are toxic to natural organisms in aqueous environments [15–20], indicating that caution is required when ILs are used for those applications. To design ILs that have low toxicity but still retain high efficiency, the mechanism for structural and dynamic effects of ILs on toxicity needs to be understood, which has motivated experi-

mental and simulation studies on the interactions between ILs and membranes.

Dependence of toxicity on the IL size has been experimentally investigated. Evans showed that imidazolium-based ILs with longer hydrocarbon tails more significantly destabilize liposomes and supported lipid bilayers [21–23]. Jeong et al. also showed that longer ILs at higher concentrations more effectively insert into membranes, which induces membrane instability, leading to the lower transition temperature of membranes [24]. Galluzzi et al. found that the surfactant – monolayer interaction can be modulated by the IL-tail length rather than by the electrostatic interactions between headgroups of ILs and lipids [25]. Also, they showed that ILs with short tails insert into the monolayer and reversibly detach from it, while relatively long ILs can only irreversibly insert. Recently, Benedetto et al. performed neutron reflectometry experiments, showing that ILs occupy the volume of ~5% and ~10%, respectively, in palmitoyloleoylglycerophosphocholine (POPC) and dimyristoylglycerophosphocholine (DMPC) bilayers [26], indicating the higher volume fraction of ILs in the membrane composed of saturated

\* Corresponding author. Tel.: +823180053569

E-mail address: [leeh@dankook.ac.kr](mailto:leeh@dankook.ac.kr)

lipids. However, the effects of membrane components on the IL insertion and bilayer size have not yet been understood, which requires the understanding of the interactions between ILs and membranes at nearly the atomic scale.

Molecular dynamics (MD) simulations have been performed to understand the interactions between imidazolium-based ionic surfactants and lipid bilayers. Ballone and coworkers simulated ionic surfactants in bilayers consisting of either cholesterol or phospholipids, showing the surfactant adsorption and the preferred position of surfactants and counterions [27,28]. Klahn and Zacharias performed free energy calculations, showing that cholesterol influence the structure and electrostatics of membranes and thus inhibit the insertion of surfactants into the bilayer [29]. Our group simulated self-assemblies of ionic surfactants of different lengths in lipid bilayers, showing the reversible interaction of short surfactants [30], in agreement with Galluzzi et al.'s experiments [25]. In particular, we found that the binding and insertion of surfactants into the bilayer can be modulated by both electrostatic and hydrophobic interactions between surfactants and bilayers, which depends on the tail length of surfactants. Recently, Benedetto et al. found that ILs with chloride ( $\text{Cl}^-$ ) ions increase the diffusivity of POPC bilayers, while those with hexafluorophosphate ( $\text{PF}_6^-$ ) ions decrease the bilayer diffusivity, showing the dependence on anions [31]. Although these simulations support the experimental observations regarding the effects of the ionic-surfactant size, charge, and cholesterol, the dependence on phospholipid types has not been computationally studied.

In this work, we therefore perform MD simulations of differently sized imidazolium-based ionic surfactants in three different phospholipid bilayers with either saturated or unsaturated hydrocarbon tails. The extent of the insertion of surfactants into bilayers and their effects on the bilayer size are analyzed, which are compared to those measured from experiments. Also, the effect of the surfactant insertion on the lateral dynamics of bilayers is investigated, which depends on the phospholipid type. These findings can explain the experimental observations that showed that ionic surfactants occupy the higher volume fraction in the saturated-phospholipid bilayer than in the unsaturated-phospholipid bilayer [26].

## 2. Methods

All simulations and analyses were performed with the GROMACS4.5.5 simulation package [32–34] with the OPLS all-atom force field (FF) and TIP4P water model [35,36]. Imidazolium-based ionic surfactants such as 1-ethyl-3-methylimidazolium ( $\text{C}_2\text{MIM}$ ), 1-butyl-3-methylimidazolium ( $\text{C}_4\text{MIM}$ ), and 1-hexyl-3-methylimidazolium ( $\text{C}_6\text{MIM}$ ) were modeled using the OPLS ionic-liquid FF developed by Sambasivaraao and Acevedo [37] (Fig. 1), which has accurately predicted the experimentally observed or theoretically derived structural and thermodynamic properties of ionic surfactants and their solvent effects on the polymer conformation [38], and thus has been widely used for many previous simulations [39–42]. For lipids, potential parameters for dimyristoylglycerophosphocholine (DMPC), palmitoyloleoylglycerophosphocholine (POPC), and dioleoylglycerophosphocholine (DOPC) were taken directly from the Berger lipid FF modified by Tieleman et al. [43,44]. We equilibrated pure bilayers without ionic surfactants, showing the area per lipid of  $62.3 \pm 1.5$ ,  $64.6 \pm 0.2$ , and  $67.7 \pm 0.2 \text{ \AA}^2$ , respectively, for DMPC, POPC, and DOPC bilayers. These are close to experimental values of  $59.9$  (DMPC),  $64.3$  (POPC), and  $67.4 \text{ \AA}^2$  (DOPC) at  $303 \text{ K}$  [45,46].

16 or 60 ionic surfactants were randomly added to the water region of the equilibrated bilayer system (Fig. 2). The final simulated system consists of 16 or 60 ionic surfactants, 128 lipids (64 lipids

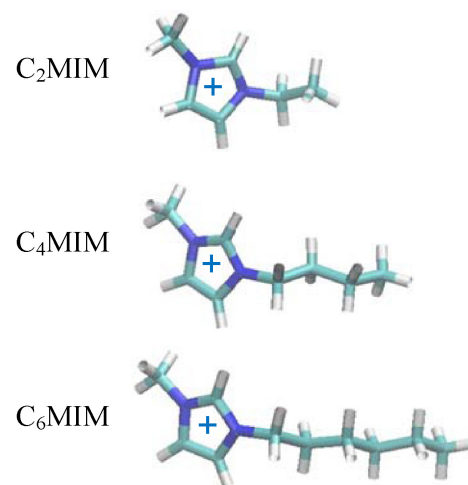


**Fig. 1.** Structures of ionic surfactants ( $\text{C}_2\text{MIM}$ ,  $\text{C}_4\text{MIM}$ , and  $\text{C}_6\text{MIM}$ ). Light-blue, blue, and white colors represent C, N, and H atoms, respectively. The images were created with Visual Molecular Dynamics [54].

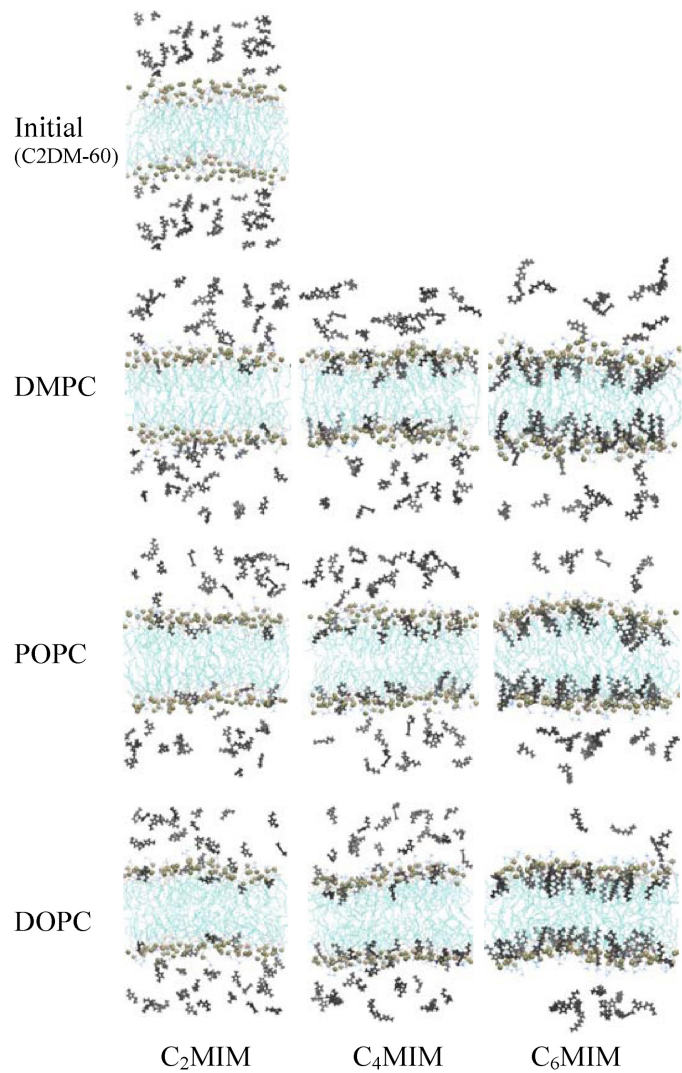


**Fig. 2.** Snapshots at the beginning (0 ns) and end (400 ns) of simulations with 60 ionic surfactants (0.38 M). Initial configuration is shown only for C2DM-60, but this random configuration is applied for all other systems. Black, brown, and light-blue colors represent ionic surfactants, lipid phosphates and hydrocarbon tails, respectively. For clarity, water and counterions are omitted. (For interpretation of the references to colour in this figure legend, the reader is referred to the web version of this article.)

per leaflet), ~8,000 water molecules, and 16 or 60 counterions ( $\text{Cl}^-$ ) in a periodic box of sizes  $6 \times 7 \times 6 \times 7 \times 9 \sim 10 \text{ nm}^3$ . Cutoffs of 14 Å and 11 Å were respectively applied for Lennard-Jones and Coulomb potentials with the inclusion of particle mesh Ewald for long-range electrostatics [47]. A pressure of 1 bar and a temperature of either 298 K (for POPC and DOPC) or 304 K (for DMPC), which are higher than the gel-to-liquid transition temperature (271, 255, and 297 K, respectively, for POPC, DOPC, and DMPC [48]) as well as correspond to experimental temperatures, were maintained by applying the velocity-rescale thermostat [49] and Berendsen barostat [50] in the  $\text{NP}_{xy}\text{P}_z\text{T}$  ensemble with the semi-isotropic pressure coupling. The LINCS algorithm was used to constrain the bond lengths [51]. Simulations were performed for 400 ns with a time step of 2 fs on computational facilities supported by the National Institute of Supercomputing and Networking/Korea Institute of Science and Technology Information with supercomputing resources including technical support (KSC-2014-C3-068). The last-100 ns trajectories were used for analyses. Note that DMPC- and POPC-bilayer systems were simulated entirely in this work, while for DOPC bilayers our previous 250 ns-long simulations were extended up to 400 ns [30].

### 3. Results and discussion

16 or 60 imidazolium-based ionic surfactants of different sizes were simulated with different phospholipid bilayers for 400 ns. Simulated systems are listed in Table 1, where “C” and the first number indicate the number of hydrocarbons in the surfactant tail. Initials “DM”, “PO”, and “DO” respectively designate DMPC, POPC, and DOPC bilayers, which are followed by the number of ionic-surfactant molecules. For example, “C2PO-16” indicates the system of 16C<sub>2</sub>MIM surfactants with the POPC bilayer.

#### 3.1. Insertion of ionic surfactants into lipid bilayers

Fig. 2 shows snapshots from the beginning (top) and end of simulations with 60 ionic surfactants in DMPC, POPC, and DOPC bilayers (rows 2–4). Ionic surfactants of 0.38 M, which were initially randomly positioned in the water region with the thickness of 6 nm, insert into lipid bilayers for all simulated systems, but their insertion extents differ. Regardless of the lipid type, C<sub>6</sub>MIMs mostly insert into lipid bilayers, while much fewer C<sub>2</sub>MIMs insert, indicating that ionic surfactants with longer hydrocarbon chains more significantly insert into lipid bilayers. To quantify this, numbers of inserted surfactants were calculated as a function of simulation time. Fig. 3 shows that for the systems with C<sub>2</sub>MIMs and C<sub>4</sub>MIMs, the numbers of inserted surfactants do not increase much and fluctuate for whole simulation time, while those values for C<sub>6</sub>MIMs drastically increase with much less fluctuation. This indicates that surfactants with short hydrocarbon tails insert into the bilayer and detach from it, while the inserted surfactants with longer tails do not reversibly interact with the bilayer, in agreement with experiments [25] and previous simulations [30]. These trends similarly occur in DMPC, POPC, and DOPC bilayers, indicating no effect of the lipid type on the insertion of surfactants. Note that Galluzzi et al.’s experiments showed that C<sub>4</sub>MIMs reversibly interact with DOPC monolayers [25], while Benedetto et al. found that C<sub>4</sub>MIMs irreversibly interact with POPC and DMPC bilayers [26], indicating the conflicting experimental results. Our simulations here showed that C<sub>4</sub>MIM reversibly interact with bilayers, but its extent of reversibility is less than C<sub>2</sub>MIM, indicating that further systematic experiments and simulation studies are required to resolve the reversible interaction between ILs and bilayers.

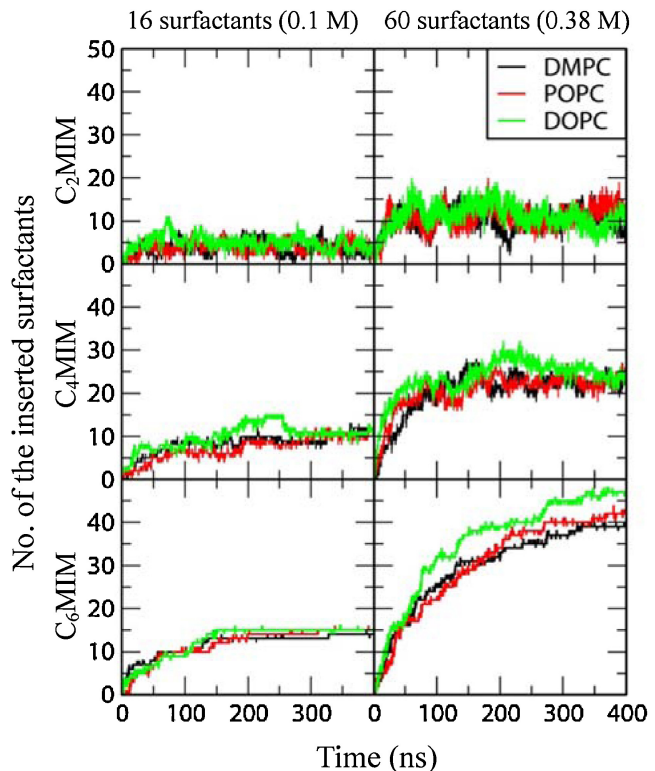


**Fig. 3.** Number of ionic surfactants inserted into lipid bilayers as a function of time.

#### 3.2. The effects of ionic surfactants on the bilayer thickness and surface size

To understand the effects of ionic surfactants on the bilayer thickness and size, mass densities and bilayer-surface sizes were calculated. In Fig. 4, mass density profiles of ionic surfactants and lipids show that surfactant heads and tails overlap, respectively, with lipid phosphate and tail regions, indicating that the inserted surfactants have the electrostatic and hydrophobic interactions with lipids, as expected. The density peaks for C<sub>6</sub>MIM are higher than those for shorter ones, indicating more insertion of larger surfactants, consistent with Figs. 2 and 3. The heights of peaks for the same-sized surfactants are almost same for different lipid bilayers, again indicating no effect of the lipid type. The distances between phosphates of each leaflet are larger for POPC and DOPC bilayers than for DMPC bilayers, since POPC and DOPC lipids consist of longer unsaturated tails, leading to thicker bilayers. In particular, when surfactants are added, the peaks for lipid phosphates are only slightly shifted to the bilayer inside. This indicates that the insertion of surfactants only slightly reduces the bilayer thickness, as also observed from Benedetto et al.’s experiments that showed that when C<sub>4</sub>MIMs were added, the bilayer thickness decreased by only ~1 Å regardless of the lipid type, indicating that the inserted surfactants do not significantly influence the bilayer thickness [26].

Sizes of the bilayer surface (xy dimension) were calculated as a function of time. In Fig. 5, as surfactants insert into the bilayer, bilayer sizes increase and reach steady-state values within 300 ns, indicating that simulations are equilibrated within the simulated time scale. Bilayer sizes more significantly increase for the systems with 60 surfactants than for those with 16 surfactants, apparently because more surfactants are inserted at higher concentrations. For the systems with 60 surfactants, longer surfactants induce the larger bilayer size because they more effectively insert and thus occupy more space inside the bilayer. Also, note that the extent of the size increase is almost same in DMPC, POPC, and DOPC bilayers.

**Table 1**

List of simulations. For DOPC bilayers, our previous 250 ns-long simulations were extended up to 400 ns [30].

Surfactant type	Bilayer type	Name	No. of surfactants	Molar conc. of surfactants (M)
C <sub>2</sub> MIM	DMPC	C2DM-16	16	0.10
		C2DM-60	60	0.38
	POPC	C2PO-16	16	0.10
		C2PO-60	60	0.38
	DOPC	C2DO-16	16	0.10
		C2DO-60	60	0.38
C <sub>4</sub> MIM	DMPC	C4DM-16	16	0.10
		C4DM-60	60	0.38
	POPC	C4PO-16	16	0.10
		C4PO-60	60	0.38
	DOPC	C4DO-16	16	0.10
		C4DO-60	60	0.38
C <sub>6</sub> MIM	DMPC	C6DM-16	16	0.10
		C6DM-60	60	0.38
	POPC	C6PO-16	16	0.10
		C6PO-60	60	0.38
	DOPC	C6DO-16	16	0.10
		C6DO-60	60	0.38

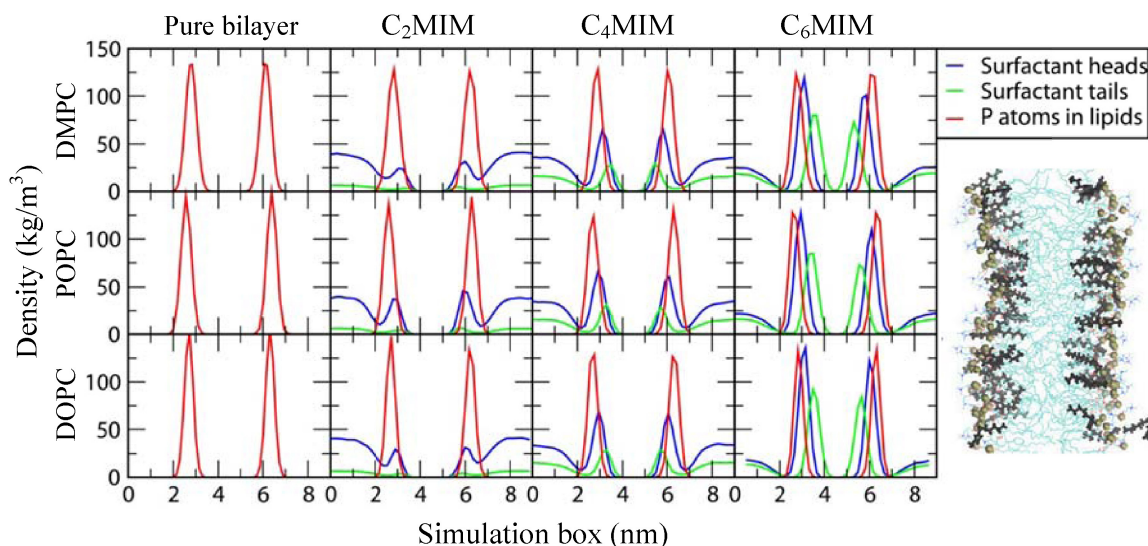


**Fig. 4.** Mass density profiles of ionic-surfactant heads (the imidazolium group) and tails, and P atoms of lipid phosphates for the bilayers with 60 ionic surfactants (0.38 M).

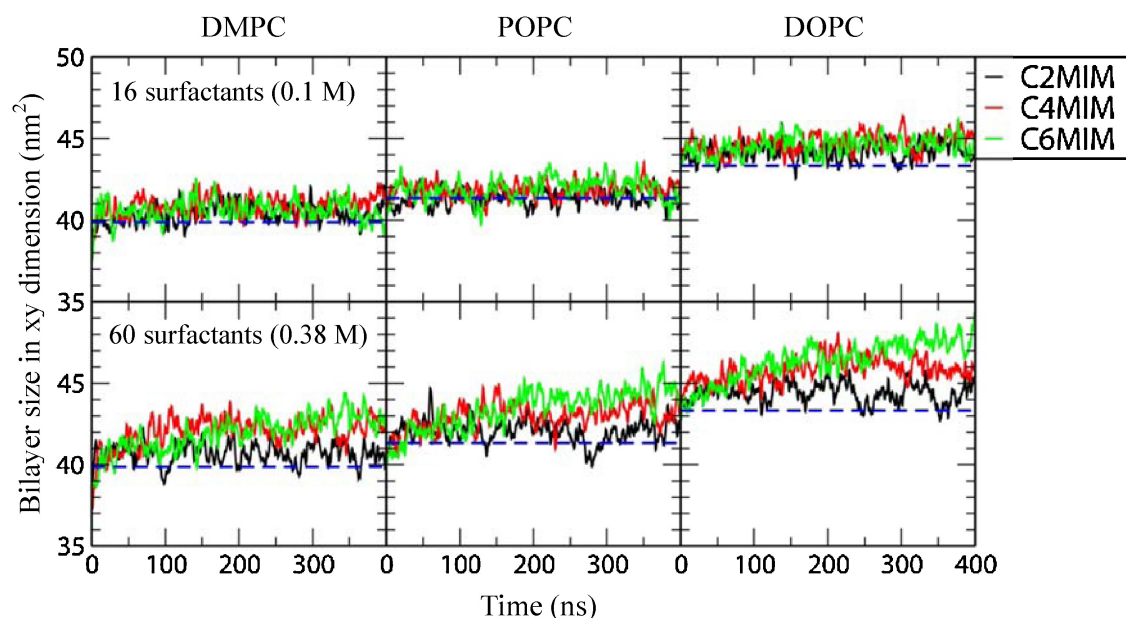


**Fig. 5.** The bilayer size in xy dimension as a function of time. For comparison, dotted blue lines represent the bilayer size for pure lipid bilayers without ionic surfactants. (For interpretation of the references to colour in this figure legend, the reader is referred to the web version of this article.)

These results indicate that ionic surfactants insert into the bilayer and increase the bilayer-surface area similarly in DMPC, POPC, and DOPC bilayers, indicating no dependence on the lipid type, which favorably compares with Benedetto et al.'s recent simulations of ILs with POPC bilayers that showed more detailed analyses of the bilayer properties such as volumes, elastic moduli, and thermal compressibility [31].

### 3.3. The volume fraction of ionic surfactants in lipid bilayers

The above-mentioned results indicate that the amount of inserted ionic surfactants and their effects on the bilayer size do not significantly differ in DMPC, POPC, and DOPC bilayers. Note that in Benedetto et al.'s experiments the C<sub>4</sub>MIM molecules occupy ~5% of the bilayer volume in the POPC bilayer and ~10% in the DMPC bilayer [26]. Since the volume fractions of surfactants significantly differ in POPC and DMPC bilayers, Benedetto et al.'s experiments seem to conflict with our simulations. To resolve this, we calculated the number of the inserted surfactants, the bilayer size in xy dimension, and the volume fraction of surfactants in the bilayer. In Fig. 6, the number of inserted surfactants and the bilayer size are higher for the systems with 60C<sub>4</sub>MIMs or C<sub>6</sub>MIMs than for other systems, apparently because of more insertion of larger surfactants at higher concentrations, consistent with Figs. 3–5. Although more surfactant insertion and larger bilayer size are observed for 60C<sub>6</sub>MIM in POPC and DOPC bilayers than for those in DMPC bilayer, volume fractions of surfactants are higher in the DMPC bilayer than in POPC and DOPC bilayers. This is presumably because the same amount of inserted surfactants yields different extents of increases in the bilayer volume. Note that areas per lipid of pure DMPC, POPC, and DOPC bilayers are  $62.3 \pm 1.5$ ,  $64.6 \pm 0.2$ , and  $67.7 \pm 0.2 \text{ \AA}^2$ , respectively. Since the area per lipid for DMPC bilayer is smaller than those for POPC and DOPC bilayers, the same amount of inserted lipids should induce relatively higher volume fractions in DMPC bilayer than in POPC and DOPC bilayers. In particular, Fig. 6 (bottom) shows that volume fractions of C<sub>4</sub>MIM are 4.6% and 8.7% respectively in POPC and DMPC bilayers, close to experimental values of ~5% and ~10% [26], indicating that simulations can reproduce experimental observations regarding the effect of the ionic-surfactant insertion on the bilayer volume.

### 3.4. Dependence of lateral mobility on the phospholipid type

Although the extent of the surfactant insertion and its effect on bilayer size are similar for different bilayers, its effect on the lateral mobility of bilayers may depend on the lipid type. To investigate this, lateral diffusion coefficients of lipids were calculated from the slopes of the mean-square displacements (MSD) in the xy-plane (the direction perpendicular to the bilayer normal). Here, lateral diffusion coefficients of pure lipid bilayers without surfactants were also calculated, showing  $0.81 (\pm 0.07)$ ,  $0.7 (\pm 0.1)$ , and  $0.74 (\pm 0.1) \times 10^{-7} \text{ cm}^2/\text{s}$ , respectively, for DMPC, POPC, and DOPC bilayers, which favorably compare with experimental values of  $1.0$ ,  $0.78$ , and  $0.82 \times 10^{-7} \text{ cm}^2/\text{s}$  [52,53]. Fig. 7 shows that ionic surfactants increase lateral diffusivities of all simulated bilayers, but their extents differ. The presence of ionic surfactants drastically increases the lateral diffusivity of DMPC bilayer, while lateral diffusivities of POPC and DOPC bilayers only slightly increase. In particular, for DMPC bilayers, C<sub>6</sub>MIMs more significantly increase lateral diffusivity than do C<sub>2</sub>MIM and C<sub>4</sub>MIM, indicating that longer surfactants can more effectively increase the bilayer mobility. This effect of C<sub>6</sub>MIMs occurs in the DMPC bilayer, but not in POPC and DOPC bilayers, indicating that the effect of surfactants on the bilayer mobility depends on the bilayer type. These results agree with Benedetto et al.'s recent simulations that showed the increased bilayer diffusivity in the presence of Cl<sup>-</sup> ions [31]. Note that they

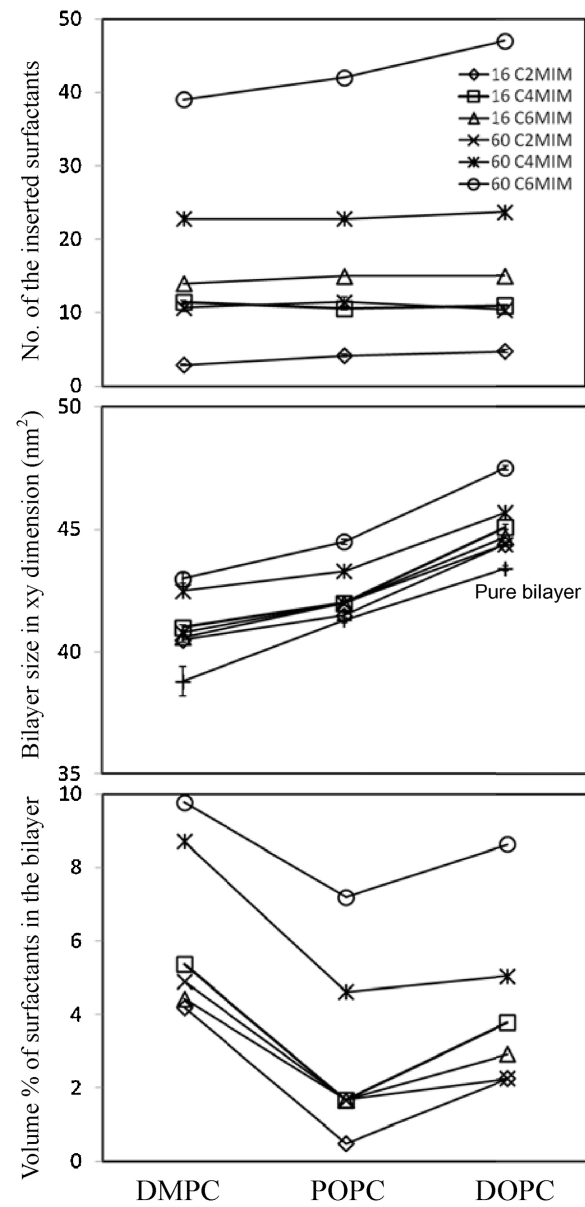


**Fig. 6.** Number of the inserted surfactants at the end of simulations (top), average bilayer size in xy dimension (middle), and the percentage of surfactants in the bilayer volume (bottom). Errors are within 0.5.

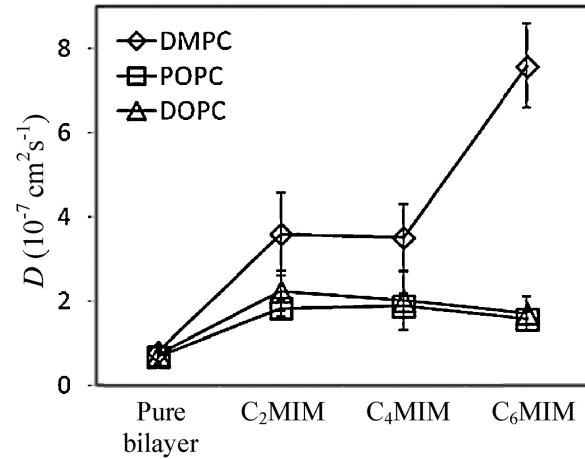


**Fig. 7.** Lateral diffusion coefficients of lipids for the bilayers with 60 ionic surfactants (0.38 M).

also found that  $\text{PF}_6^-$  ions reduce the bilayer diffusivity [31], which is opposite to the effect of  $\text{Cl}^-$  ions. These opposite effects of anions on the bilayer dynamics have not yet been explained, which motivates more systematic experiments and simulation studies.

These findings indicate that the insertion of ionic surfactants into the bilayer and its effect on the bilayer size do not depend on the bilayer type, while the bilayer dynamics is significantly influenced by the bilayer type. The changes of the volume fraction of ionic surfactants in the bilayer agree well with experimental values, which can be explained by our findings that the same concentration of ionic surfactants yields more increases in the volume fraction of surfactants in the bilayer with the smaller area per lipid. Insertion of ionic surfactants increases the lateral mobility more significantly for DMPC bilayers than for POPC and DOPC bilayers, presumably because shorter saturated DMPC lipids can be more easily disordered by surfactants than do longer unsaturated POPC and DOPC lipids. These indicate that the effects of ionic surfactants on the bilayer mobility depend on the lipid type, which should be further checked by experiments.

#### 4. Conclusions

We performed 400 ns-long MD simulations of imidazolium-based ionic surfactants with three different bilayers composed of DMPC, POPC, and DOPC lipids. Ionic surfactants, which were initially randomly positioned in the solvent region outside the bilayer, insert into the bilayer and increase the bilayer-surface area, which occur more significantly for longer surfactants at higher concentrations regardless of the lipid type of bilayers. Also, short surfactants insert into the bilayer and then reversibly detach from it, while long surfactants can only insert, as observed in experiments and previous simulations. The inserted surfactants only slightly decrease the bilayer thickness, favorably compared with experiments. These indicate that the insertion of surfactants and its effects on the bilayer size and thickness do not depend on the lipid type, which seems to conflict with recent experiments that showed that ionic surfactants occupy more space in the DMPC bilayer than in the POPC bilayer. To examine this, we calculated the volume fraction of surfactants in the bilayer, showing that surfactants occupy the larger volume fraction in DMPC bilayers than in POPC and DOPC bilayers, apparently because pure DMPC bilayer has the smaller area per lipid, and hence the same amount of inserted surfactants should yield the higher extent of an increase in the bilayer size for the DMPC bilayer than for POPC and DOPC bilayers. In particular, volume fractions of C<sub>4</sub>MIM surfactants are 4.6% and 8.7%, respectively, in POPC and DMPC bilayers, close to experimental values of 5% and 10%. DMPC bilayers do not only show the higher volume fraction of surfactants but also show the higher lateral diffusivity, indicating the significant effects on the bilayer mobility. Our simulation findings indicate that the effects of ionic surfactants on the bilayer dynamics depend on the phospholipid type, as well as explain the experimental observations that showed the different volume fractions of surfactants in POPC and DMPC bilayers.

#### References

- [1] J.S. Wilkes, A short history of ionic liquids – from molten salts to neoteric solvents, *Green Chem.* 4 (2002) 73–80.
- [2] P. Wasserscheid, Chemistry, volatile times for ionic liquids, *Nature* 439 (2006) 797.
- [3] M.J. Earle, J.M.S.S. Esperança, M.A. Gilea, J.N.C. Lopes, L.P.N. Rebelo, J.W. Magee, et al., The distillation and volatility of ionic liquids, *Nature* 439 (2006) 831–834.
- [4] T. Ueki, M. Watanabe, Macromolecules in ionic liquids: progress, challenges, and opportunities, *Macromolecules* 41 (2008) 3739–3749.
- [5] N.V. Plechkova, K.R. Seddon, Applications of ionic liquids in the chemical industry, *Chem. Soc. Rev.* 37 (2008) 123–150.
- [6] Z. Conrad Zhang, Catalysis in ionic liquids, In: *Adv. Catal.* 49 (2006) 153–237.
- [7] T. Welton, Ionic liquids in catalysis, *Coord. Chem. Rev.* 248 (2004) 2459–2477.
- [8] H. Saruwatari, T. Kuboki, T. Kishi, S. Mikoshiba, N. Takami, Imidazolium ionic liquids containing LiBOB electrolyte for lithium battery, *J. Power Source* 195 (2010) 1495–1499.
- [9] T. Kuboki, T. Okuyama, T. Ohsaki, N. Takami, Lithium-air batteries using hydrophobic room temperature ionic liquid electrolyte, *J. Power Sources* 146 (2005) 766–769.
- [10] X. Han, D.W. Armstrong, Ionic liquids in separations, *Acc. Chem. Res.* 40 (2007) 1079–1086.
- [11] M. Smiglak, A. Metlen, R.D. Rogers, The second evolution of ionic liquids: from solvents and separations to advanced materials – energetic examples from the ionic liquid cookbook, *Acc. Chem. Res.* 40 (2007) 1182–1192.
- [12] Y. He, Z. Li, P. Simone, T.P. Lodge, Self-assembly of block copolymer micelles in an ionic liquid, *J. Am. Chem. Soc.* 128 (2006) 2745–2750.
- [13] T.P. Lodge, Materials science: a unique platform for materials design, *Science* 321 (2008) 50–51.
- [14] R. Rinaldi, R. Palkovits, F. Schüth, Depolymerization of cellulose using solid catalysts in ionic liquids, *Angew. Chem. – Int. Ed.* 47 (2008) 8047–8050.
- [15] A. Latała, P. Stepnowski, M. Nędzi, W. Mrozik, Marine toxicity assessment of imidazolium ionic liquids: acute effects on the Baltic algae *Oocystis submarina* and *Cyclotella meneghiniana*, *Aquat. Toxicol.* 73 (2005) 91–98.
- [16] R.J. Bernot, M.A. Brueske, M.A. Evans-White, G.A. Lamberti, Acute and chronic toxicity of imidazolium-based ionic liquids on *Daphnia magna*, *Environ. Toxicol. Chem.* 24 (2005) 87–92.
- [17] J. Pernak, K. Sobaszkiewicz, I. Mirska, Anti-microbial activities of ionic liquids, *Green Chem.* 5 (2003) 52–56.
- [18] C. Pretti, C. Chiappe, D. Pieraccini, M. Gregori, F. Abramo, G. Monni, et al., Acute toxicity of ionic liquids to the zebrafish (*Danio rerio*), *Green Chem.* 8 (2006) 238–240.
- [19] R.P. Swatoski, J.D. Holbrey, R.D. Rogers, Ionic liquids are not always green: hydrolysis of 1-butyl-3-methylimidazolium hexafluorophosphate, *Green Chem.* 5 (2003) 361–363.
- [20] M. Petkovic, K.R. Seddon, L.P.N. Rebelo, C. Silva Pereira, Ionic liquids: a pathway to environmental acceptability, *Chem. Soc. Rev.* 40 (2011) 1383–1403.
- [21] K.O. Evans, Supported phospholipid bilayer interaction with components found in typical room-temperature ionic liquids – a QCM-D and AFM study, *Int. J. Mol. Sci.* 9 (2008) 498–511.
- [22] K.O. Evans, Supported phospholipid membrane interactions with 1-butyl-3-methylimidazolium chloride, *J. Phys. Chem. B* 112 (2008) 8558–8562.
- [23] K.O. Evans, Room-temperature ionic liquid cations act as short-chain surfactants and disintegrate a phospholipid bilayer, *Colloids Surfaces A: Physicochem. Eng. Aspects* 274 (2006) 11–17.
- [24] S. Jeong, S.H. Ha, S.H. Han, M.C. Lim, S.M. Kim, Y.R. Kim, et al., Elucidation of molecular interactions between lipid membranes and ionic liquids using model cell membranes, *Soft Matter* 8 (2012) 5501–5506.
- [25] M. Galluzzi, S. Zhang, S. Mohamadi, A. Vakurov, A. Podestà, A. Nelson, Interaction of imidazolium-based room-temperature ionic liquids with DOPC phospholipid monolayers: electrochemical study, *Langmuir* 29 (2013) 6573–6581.
- [26] A. Benedetto, F. Heinrich, M.A. Gonzalez, G. Fragneto, E. Watkins, P. Ballone, Structure and stability of phospholipid bilayers hydrated by a room-temperature ionic liquid/water solution: a neutron reflectometry study, *J. Phys. Chem. B* 118 (12) (2014) 192–206.
- [27] S.R.T. Cromie, M.G. Del Pópolo, P. Ballone, Interaction of room temperature ionic liquid solutions with a cholesterol bilayer, *J. Phys. Chem. B* 113 (11) (2009) 642–648.
- [28] R.J. Bingham, P. Ballone, Computational study of room-temperature ionic liquids interacting with a POPC phospholipid bilayer, *J. Phys. Chem. B* 116 (11) (2012) 20.
- [29] M. Klähn, M. Zacharias, Transformations in plasma membranes of cancerous cells and resulting consequences for cation insertion studied with molecular dynamics, *Phys. Chem. Chem. Phys.* 15 (2013) 14427–14441.
- [30] H. Lee, T.J. Jeon, THe binding and insertion of imidazolium-based ionic surfactants into lipid bilayers: the effects of surfactant size and salt concentration, *Phys. Chem. Chem. Phys.* 17 (2015) 5725–5733.
- [31] A. Benedetto, R.J. Bingham, P. Ballone, Structure and dynamics of POPC bilayers in water solutions of room temperature ionic liquids, *J. Chem. Phys.* 142 (2015) 124706.
- [32] D. Van Der Spoel, E. Lindahl, B. Hess, G. Groenhof, A.E. Mark, H.J.C. Berendsen, GROMACS fast, flexible, and free, *J. Comput. Chem.* 26 (2005) 1701–1718.
- [33] E. Lindahl, B. Hess, D. van der Spoel, GROMACS 3.0: a package for molecular simulation and trajectory analysis, *J. Mol. Model.* 7 (2001) 306–317.
- [34] B. Hess, C. Kutzner, D. van der Spoel, E. Lindahl, GROMACS 4: algorithms for highly efficient, load-balanced, and scalable molecular simulation, *J. Chem. Theory Comput.* 4 (2008) 435–447.
- [35] G.A. Kaminski, R.A. Friesner, J. Tirado-Rives, W.L. Jorgensen, Evaluation and reparametrization of the OPLS-AA force field for proteins via comparison with accurate quantum chemical calculations on peptides, *J. Phys. Chem. B* 105 (2001) 6474–6487.
- [36] W.L. Jorgensen, D.S. Maxwell, J. Tirado-Rives, Development and testing of the OPLS all-atom force field on conformational energetics and properties of organic liquids, *J. Am. Chem. Soc.* 118 (1996) 11225–11236.
- [37] S.V. Sambasivaraao, O. Acevedo, Development of OPLS-AA force field parameters for 68 unique ionic liquids, *J. Chem. Theory Comput.* 5 (2009) 1038–1050.

- [38] J. Mondal, E. Choi, A. Yethiraj, Atomistic simulations of poly(ethylene oxide) in water and an ionic liquid at room temperature, *Macromolecules* 47 (2014) 438–446.
- [39] T. Méndez-Morales, J. Carrete, M. Pérez-Rodríguez, Ó. Cabeza, L.J. Gallego, R.M. Lynden-Bell, et al., Molecular dynamics simulations of the structure of the graphene-ionic liquid/alkali salt mixtures interface, *Phys. Chem. Chem. Phys.* 16 (2014) 13271–13278.
- [40] B. Docampo-Álvarez, V. Gómez-González, T. Méndez-Morales, J. Carrete, J.R. Rodríguez, Ó. Cabeza, et al., Mixtures of protic ionic liquids and molecular cosolvents: a molecular dynamics simulation, *J. Chem. Phys.* 140 (2014).
- [41] J. Carrete, T. Méndez-Morales, M. García, J. Vila, O. Cabeza, L.J. Gallego, et al., Thermal conductivity of ionic liquids: a pseudolattice approach, *J. Phys. Chem. C* 116 (2012) 1265–1273.
- [42] T. Méndez-Morales, J. Carrete, S. Bouzón-Capelo, M. Pérez-Rodríguez, O. Cabeza, L.J. Gallego, et al., MD simulations of the formation of stable clusters in mixtures of alkaline salts and imidazolium-based ionic liquids, *J. Phys. Chem. B* 117 (2013) 3207–3220.
- [43] D.P. Tieleman, J.L. MacCallum, W.L. Ash, C. Kandt, Z. Xu, L. Monticelli, Membrane protein simulations with a united-atom lipid and all-atom protein model: lipid-protein interactions, side chain transfer free energies and model proteins, *J. Phys. Condens. Matter* 18 (2006) S1221–S1234.
- [44] E. Han, H. Lee, Effect of the structural difference between Bax- $\alpha$ 5 and Bcl-xL- $\alpha$ 5 on their interactions with lipid bilayers, *Phys. Chem. Chem. Phys.* 16 (2014) 981–988.
- [45] N. Kučerka, J.F. Nagle, J.N. Sachs, S.E. Feller, J. Pencer, A. Jackson, et al., Lipid bilayer structure determined by the simultaneous analysis of neutron and X-ray scattering data, *Biophys. J.* 95 (2008) 2356–2367.
- [46] N. Kučerka, M.P. Nieh, J. Katsaras, Fluid phase lipid areas and bilayer thicknesses of commonly used phosphatidylcholines as a function of temperature, *Biochimica Biophysica Acta – Biomembrane* 1808 (2011) 2761–2771.
- [47] U. Essmann, L. Perera, M.L. Berkowitz, T. Darden, H. Lee, L.G. Pedersen, A smooth particle mesh ewald method, *J. Chem. Phys.* 103 (1995) 8577–8593.
- [48] R. Koynova, M. Caffrey, Phases and phase transitions of the phosphatidylcholines, *Biochimica Biophysica Acta-Rev. Biomembranes* 1376 (1998) 91–145.
- [49] G. Bussi, D. Donadio, M. Parrinello, Canonical sampling through velocity rescaling, *J. Chem. Phys.* 126 (2007) 014101.
- [50] H.J.C. Berendsen, J.P.M. Postma, W.F. van Gunsteren, A. DiNola, J.R. Haak, Molecular-dynamics with coupling to an external bath, *J. Chem. Phys.* 81 (1984) 3684–3690.
- [51] B. Hess, P-LINCS a parallel linear constraint solver for molecular simulation, *J. Chem. Theory Comput.* 4 (2008) 116–122.
- [52] A. Filippov, G. Orädd, G. Lindblom, The effect of cholesterol on the lateral diffusion of phospholipids in oriented bilayers, *Biophys. J.* 84 (2003) 3079–3086.
- [53] G. Orädd, G. Lindblom, NMR studies of lipid lateral diffusion in the DMPC/gramicidin D/water system: peptide aggregation and obstruction effects, *Biophys. J.* 87 (2004) 980–987.
- [54] W. Humphrey, A. Dalke, K. Schulten, VMD Visual molecular dynamics, *J. Mol. Graphics* 14 (1996) 33–38.